



# Automated Detection Of Masses And Microcalcifications In Pectoral Removed Mlo Mammograms With Image Enhancement And Modified Fuzzy C-Mean

<sup>1</sup>Ch. Sarada, <sup>2</sup>Dr K. Vijaya Lakshmi, <sup>3</sup>Prof. M.PADMAVATHAMMA

<sup>1</sup>Research Scholar, Computer Science, Sri Venkateswara University, Tirupati, AP, India.

<sup>1</sup>Sr.Asst.Professor ,CSE, CVR College of Engineering, Hyderabad, Telangana, India.

<sup>2</sup>Assistant Professor, Computer Science, Sri Venkateswara University, Tirupati, AP, India.

<sup>3</sup>Professor and Principal, Computer Science, Sri Venkateswara University, Tirupati, AP, India.

**Abstract:** Cancer disease occurs when cells divide abnormally and invade nearby tissues. Breast cancer is one fatal disease where breast cells like duct cells and milk gland cells grow uncontrollably. If Cancer is not recognised in the early stage, it leads to loss of life. Mammography is one kind of efficient breast screening to detect abnormalities at the early stage. Abnormalities detected through Mammography may suspect breast cancer or recommend further screening. Microcalcifications and masses are the indicators of breast cancer in MLO Mammograms. Detection of both masses and microcalcifications in MLO Mammography is challenging work, and the presence of pectoral muscle makes this detection task further difficult. Various researchers developed procedures to detect masses from MLO Mammogram. However, all literature surveyed systems are applied to detect masses or microcalcifications but not both. We designed and developed a new approach based on the modified fuzzy c means that used an intuitionistic approach with the inclusion of spatial information, i.e., Spatial intuitionistic Fuzzy C-means algorithm and Nonsubsampled Contourlet transform (NSCT) to detect masses and microcalcifications from pectoral eliminated MLO Mammograms. It is tested on the Mini-MIAS database. It improved mass detection results compared to literature-surveyed approaches and showed promising results even in microcalcification detection.

**Index Terms** - Medical image segmentation, Breast cancer, MLO Mammogram, Nonsubsampled contourlet transform · microcalcification and mass detection, Spatial Intuitionistic fuzzy C-means clustering, computer-assisted segmentation.

## I.INTRODUCTION

Different fatty, fibrous, and glandular tissues form the female breast. The breast lobes and breast ducts are part of glandular tissue. Fibrous tissue is a connective tissue that works as a connective from the skin to the chest wall. Ligaments and scar tissue consist of fibrous or supporting, or connective tissue. Fatty tissue fills the crevices between fibrous and glandular tissue. All non-fatty tissue is referred to by doctors as fibroglandular tissue [1]. Breast lobes generate milk, and ducts carry milk to the nipple. Lymph nodes are present in the entire body that help in fighting infections.

Most of the breast tissue in thick breasts is glandular or fibrous breast tissue. The dense issue appears completely white, thicker, and denser than fatty tissue. Radiologists first look at the mammogram image to diagnose breast cancer since specific lumps and microcalcifications can be seen on mammograms. Microcalcifications are visible in mammograms only. The two main warning signs of breast cancer from the mammogram are masses and microcalcifications. Masses are the lumps/tumours, and microcalcifications are the bright/white specks in the Mammogram [2].

Fig.1 shows typical MLO Mammograms with the highlight of mass and microcalcifications.

Developing a digital image processing-based CAD system to detect masses and microcalcifications is a demanding task. Many works of literature surveyed approaches use various methodologies like morphological operations, clustering techniques, thresholding-based methods, standard segmentation methods such as Watershed, Chan-Vese, and clustering techniques like Fuzzy C-means and k-means methods in Mammogram mass detection. Most of the literature surveyed concentrated on either mass detection or microcalcification detection but not on both.

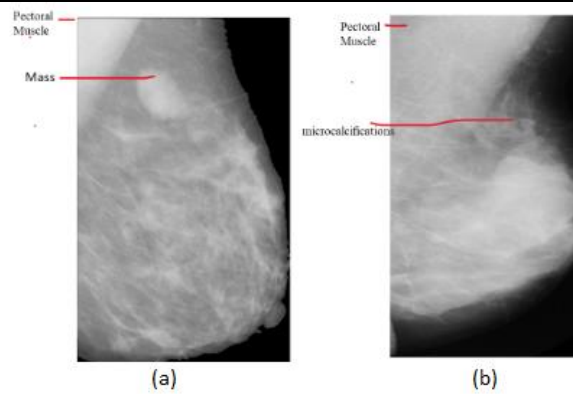


**Fig.1** MLO Mammograms with the highlight of (a) mass (b) microcalcifications

This research uses a new multistage methodology to detect masses and microcalcifications from the pectoral removed MLO mammograms. Related surveyed work is presented in section II, the proposed system is shown in section III, section IV describes the database and deals with result analysis, and finally, a conclusion and future scope are given.

## II. RELATED WORK

Vikhe et al. [13] presented an approach for mass augmentation that uses wavelet processing and the piecewise linear operator. The paper used an adaptive threshold approach to distinguish the mass from the background for mass segmentation. The suggested technique has been evaluated on 130 (45+85) pictures from two distinct databases, the DDSM and MIAS, with 91 and 90.9% True Positive Fraction rates at 2.1 and 2.35 average False Positive per image (DDSM). As far as Mini-MIAS is concerned, only 45 images are tested.

Mahfuzah et al. [14] implemented a segmentation approach based on the Chan-Vese technique. The chan-Vese procedure can do segmentation even though boundaries are not defined properly. This method is tested on just 30 DDSM images. It gave nearly 90% accurate results.

A method for mass detection from MLO mammograms using standard fuzzy C-means was proposed by Mohammed Y. Kamil et al. [15]. The accuracy of mass detection achieved is 94.12%. No specific steps were used for the detection of microcalcifications. This approach makes mass detection without removing the pectoral, contributing to additional false positives.

An approach for region detection based on the meta-heuristic Electromagnetism-like optimisation (EML) was presented by Soulami et al. [16]. This technique removes noise pixels and artefacts from the images using a Median filter; then, it separates anomalous places that use EML. This approach is vulnerable when addressing anomalies and identifying architectural deformation and calcifications in dense breasts. This method is tested on 56 Mini-MIAS images with an accuracy of 78.57%.

Hongyu et al. [17] used Gestalt psychology for Breast mass segmentation. Here, mind and behaviour are taken into consideration while detecting Breast mass. In this approach, 257 Mini-MIAS images are tested with an accuracy of 92% at a 2.215 false positive rate.

Asaad Zebari et al. [18] suggested a novel technique for separating benign from malignant breast images using mammography scans. The ROI is determined by utilising a machine learning algorithm and hybrid thresholding (ROI). The attained segmentation accuracy is 78.88%.

Ayush Shrivastava et al. [19] proposed an approach to remove pectoral muscle and detect mass by dispersed region growing algorithm from MLO mammogram. The author used the sliding window to eliminate the pectoral muscle. The accuracy achieved is 91.3%. This sliding algorithm works if the intensity in the pectoral muscle region is uniform. Otherwise, it does not work. For mass detection, region growing is applied based on distance-based seeds, where finding seeds take a lot of time.

## III. PROPOSED METHODOLOGY

The proposed system introduces a new approach based on modified fuzzy-C means that incorporates spatial information with intuitionistic fuzzy representation. This algorithm can be named Spatial Intuitionistic Fuzzy C Means (SIFCM). It also includes additional operations like enhancement using Nonsubsampled Contourlet transform, morphological operations to detect masses, and microcalcifications from pectoral removed MLO Mammogram. Fig 3.1 shows the block diagram of the proposed system.

Firstly, the breast image contains unnecessary information like labels, artefacts, black borders, and pectoral muscles. Pectoral removal is necessary to decrease false positives for mass detection as its intensity and texture levels match with masses. All the unimportant information and pectoral are removed using the procedure proposed in [3]. It is based on the ensemble approach of MSER (Maximal Stable Extremal Region) and the Slope\_Edge\_Detection method.

Fig 3.2 shows the pectoral removed along with other insignificant regions (labels, black borders).

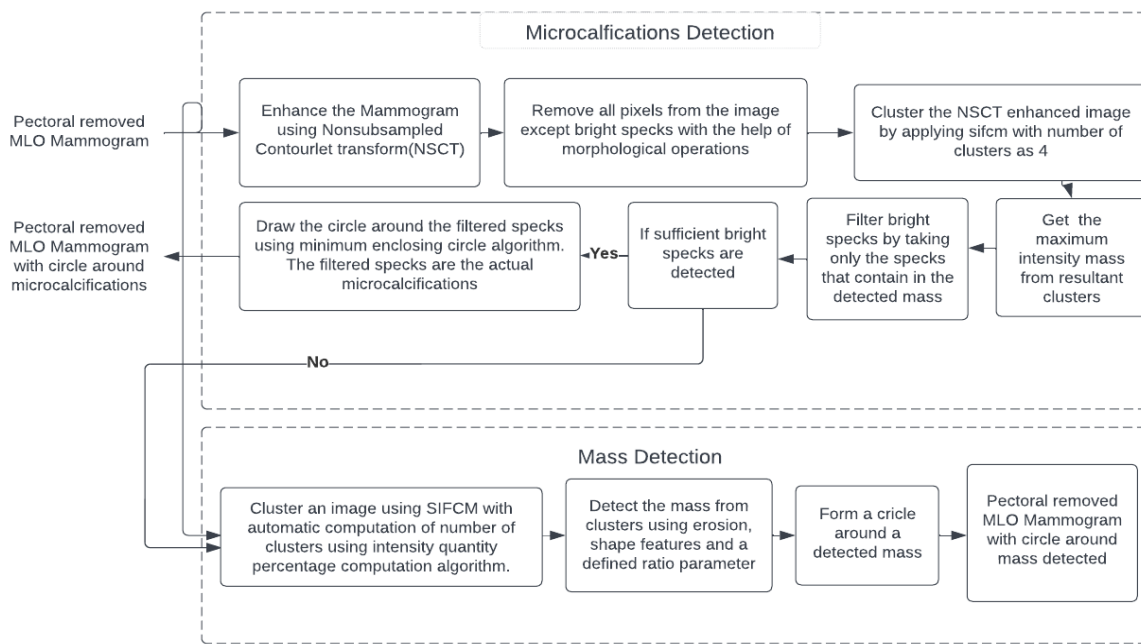


**Fig.3.1 Proposed System - Block Diagram**

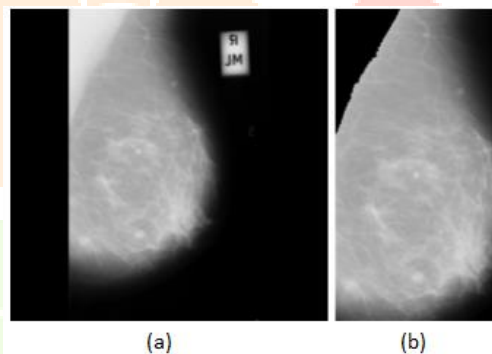


**Fig 3.2** (a) mammogram image with labels and black borders (b) pectoral, label and black borders removed image.

### 3.1 Enhancement of Image with Nonsubsampled Contourlet transform (NSCT)

The image quality should be enhanced to detect microcalcifications, as they are tiny spots which become unnoticeable if the masses surrounding them have a similar intensity range. For this purpose, Nonsubsampled Contourlet Transform [4] is employed. As per Jose et al. [4] paper, NSCT enhances microcalcifications with the increased visual appearance of bright specks. The NSCT can reduce noise while enhancing contrast and capturing good geometrical information. This is a significant advantage compared to other enhancement techniques.

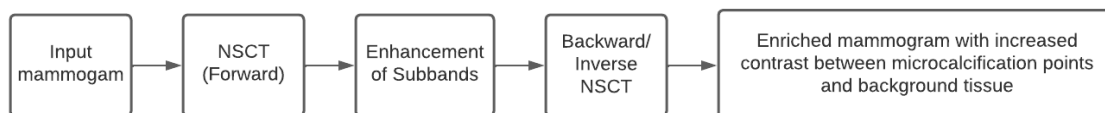


**Fig 3.3 Mammogram Enhancement using NSCT**

The simple block diagram for the mammogram image processing using NSCT is shown in Fig 3.3. The main idea is based on Jose Manuel et al. paper [4]. The pectoral removed image from the previous stage is used as the system's input; this image is then translated into the NSCT domain to produce multidirectional level decomposition.

Sample pectoral removed mammogram and its enhanced version with NSCT are demonstrated in figure 3.4.

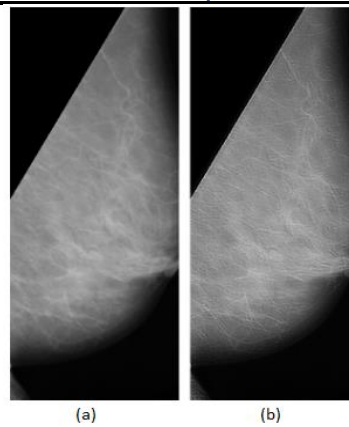


**Fig.3.4** (a) Pectoral removed MLO Mammogram (b) Enhanced image.

NSCT is applied on the whole pectoral removed image. The difference between Jose et al. [4] paper's approach and this method are that NSCT is applied for the entire image, whereas [4] applies on manually selected ROI, and the threshold levels are changed in the processing of subbands. To appreciate the difference, particularly in the Microcalcification region, Fig 3.5 shows a more visual difference in microcalcification enhancement; taking the microcalcification region of both the images, we can observe that the microcalcification (MC) points have been enriched a lot where the MC points have increased the intensity.

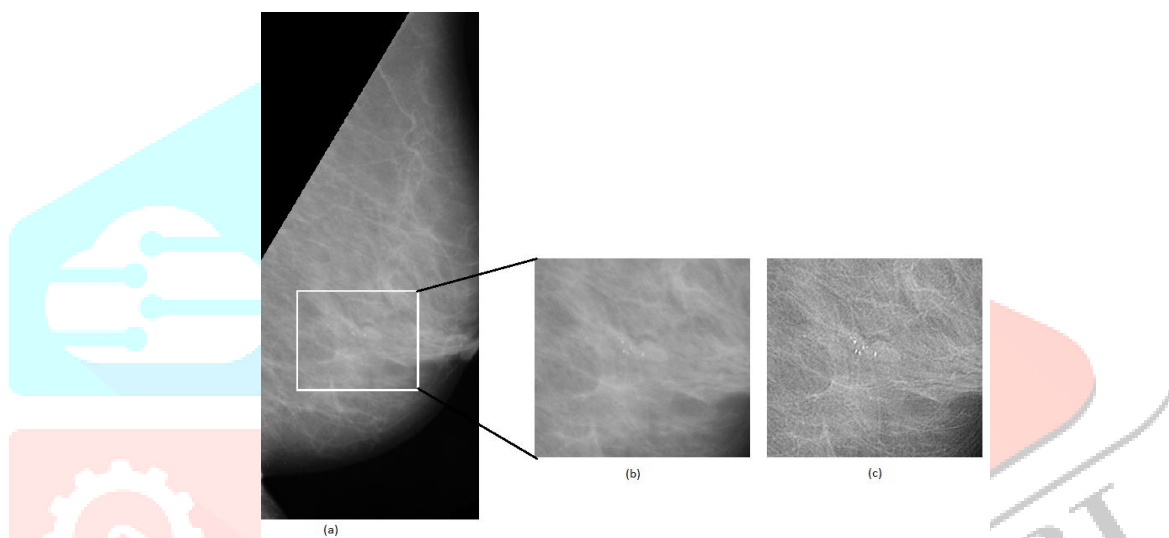


**Fig 3.5:** (a) Pectoral removed mammogram with the highlight of microcalcification region  
(b) Microcalcification region in the original image (c) Microcalcification region after applying NSCT.

Without NSCT, detecting microcalcifications (MC) becomes very difficult; applying NSCT makes detecting MC points more straightforward and can be carried out simpler by morphological operations.

### 3.2 Bright Spots (Microcalcification Points) Detection by Morphological Analysis

The next step is to extract bright specks, i.e., MC points, from the NSCT resultant image. Morphological processing based on non-flat (grayscale) structuring elements [5] is used to isolate bright spot locations from the remaining background breast tissue. detailed steps of bright spot detection are described in the following algorithm.

#### Algorithm: Extraction\_Bright\_Specks

1. Read an NCST-enhanced MLO Mammogram.
2. Form a small-size kernel with a structuring element that is not flat.
3. Dilate the image with the kernel defined in 2nd step.
4. Enhance bright objects of interest in a relatively darker background on the original image using the top hat transform. Likewise, enhance dark spots in a brighter background using black hat transform.
5. Add the top-hat transformed image to the original image.
6. Subtract the resultant image of step 5 from the black-hat-transformed image to get high contrast.
7. Subtract the image resulting from step 6 from the dilated image of step 3 to remove the background.
8. Apply thresholding operation on the image obtained from step 7 with the range of 90 to 255.
9. The resultant image is the image with only bright points.

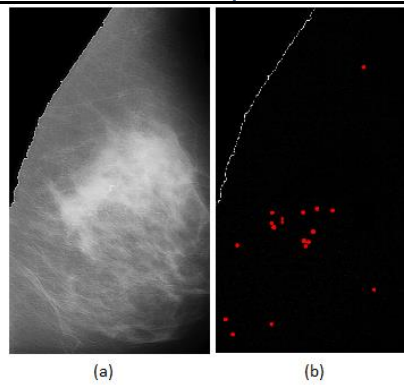


**Fig.3.6.** (a) Enhanced image with NSCT (b) After bright sport detection with morphological operations

In Fig.3.6, detected dots are shown in red with more radius for visibility. The pectoral edge also gets detected due to enhancement near the pectoral border by NSCT. As shown in (b), some dots other than the microcalcification region get detected. It is due to the brightening of spots near the breast edge border and some noise. These extra dots are removed by filtering with SIFCM.

The largest mass obtained in the cluster is taken, the points present only in this largest region are taken, and all the other points are removed from the bright\_spot\_detected image.

The figures, Fig-3.7(1) and Fig-3.7(2), demonstrate these steps.

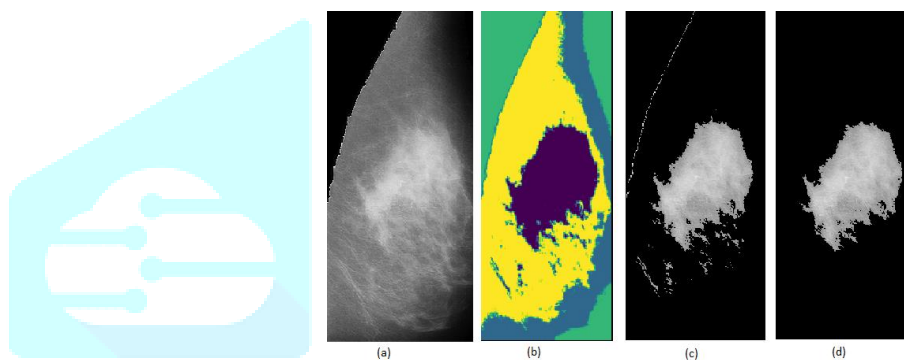


**Fig-3.7(1):** Extraction of the region by SIFCM

- (a) NSCT-enhanced image (b) SIFCM applied image  
(c) Extract the cluster which contains the highest intensity point (d) Get the largest mass region of the cluster

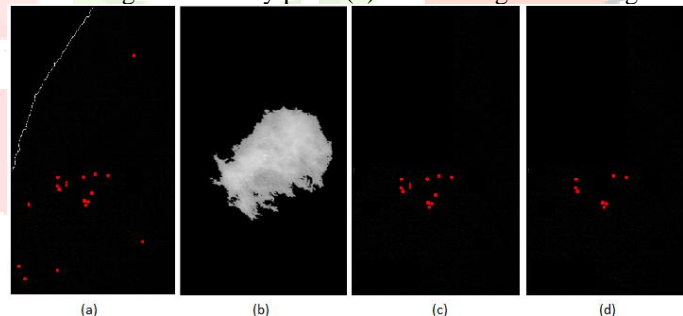


**Fig-3.7(2) -** Finding Microcalcification points after filtering by SIFCM

- (a) The thresholded image obtained from the Extraction\_bright\_spots algorithm (b) SIFCM mass (fig 3.7(1)(d))  
(c) White spots image from the thresholded image  
(d) Filtered spots image

After getting the white spots that are in the SIFCM mass (as in fig 3.7(2)(c)), a further check is carried out to remove any other extra spots. We extracted the locations of the white spots of the image (like in fig 3.7(2)(c)) and checked the intensity variation between the NSCT-enhanced and the original image at those locations. After experimental tests with images having microcalcifications and no microcalcifications, the threshold of 15 is selected. This is depicted in Fig 3.7(2)(d), where some spots got deleted compared to fig 3.7(2)(c). The threshold value of 15 is mainly selected because the NSCT enhances the microcalcification spots to a greater extent than some unimportant white spots (like noise near edges). These insignificant spots can be removed with this threshold.

If the number of spots of the final obtained image (like in Fig 3.7(2)(d)) is greater than at least 2, the image is decided to have microcalcifications, or else it does not have microcalcifications and is further given for mass detection (described in section 3.3).

This procedure is also helpful for the binary classification of images into microcalcification and not having microcalcification. Microcalcification spots in the image are best enhanced by NSCT, without which the detection becomes very difficult.



Finally, the white spots obtained, i.e., microcalcification spots, are encircled with the minimum enclosing circle algorithm. By using the location of the white spots obtained, we can compute the minimum radius and centre of the circle that can enclose these spots by Welzl's recursive algorithm [6]. It is faster compared to other enclosing circle methods.

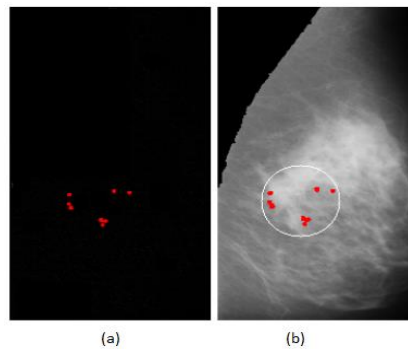


**Fig 3.8:** (a) Image of Detected Microcalcification Points (b) Minimum enclosing circle with Welzl's recursive algorithm around the detected microcalcification points (imposed the red dots of (a) on the breast image)

After the microcalcification detection, the images that resulted without any microcalcification by this algorithm are further processed for masses detection. Here masses are small or big regions, and microcalcifications are tiny bright specks. The processing of these two should be dealt with separately as microcalcifications are points and masses are regions.

The 3.3 section describes Mass detection based on the clustering algorithm - Spatial Intuitionistic Fuzzy C Means (SIFCM).

### 3.3 Detection of Masses by SIFCM with an adaptive number of clusters after image enhancement

The image should be significantly enhanced for mass detection, particularly around the masses (most tumour masses are white with a less grey-level neighbourhood). If the masses appear brighter, the SIFCM algorithm can detect these masses easily.

#### 3.3.1 Image enhancement using Wavelet-domain Homomorphic Filter and CLAHE

The NSCT enhancement is only specific to microcalcification/bright spots, as the threshold was calculated based on the intensity levels of bright spots appearing over a homogeneous background. It does not enhance masses, and different subband processing is required for mass enhancement, which is very challenging. Thus, a simpler algorithm is used based on Wen's [7] paper. The enhancement and detection are dealt with differently for masses and microcalcifications as the characteristics significantly differ for both.

An image enrichment technique using a wavelet domain homomorphic filter and CLAHE (contrast limited adaptive histogram equalisation)[7] is utilised to enhance the mass texture detail effectively, increase the contrast and brightness, and reduce noise better than the standard conventional enhancement algorithms.

The idea of this algorithm is based on Wen's [7] paper with modifications that were made suitable for mammograms. The changes made are using the bior4.4 wavelet in the discrete wavelet transform instead of 'db4' and using Butterworth low pass filter for homomorphic filtering and changing the threshold selection rule based on the soft threshold estimator's SURE (Stein's Unbiased Risk Estimate) [8]. Fig 3.9 shows the enhanced image after applying the wavelet domain homomorphic filter and CLAHE.

This enhancement method is critical for clustering algorithms to divide images into cluster regions. After enhancement, the clusters formed by SIFCM were good enough to isolate the masses.

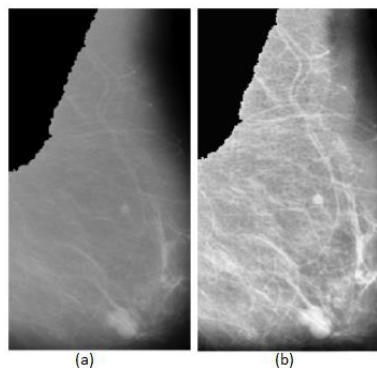


**Fig-3.9** Mammogram Enhancement using CLAHE and wavelet domain homomorphic filtering  
(a) Original pectoral removed image (b) Final enhanced image

#### 3.3.2 SIFCM with the adaptive number of clusters and Mass detection by filtering

Clustering is one of the most often used techniques for segmenting images. The two most well-known examples of cutting-edge clustering techniques are the K-means and fuzzy c-means. The fuzzy c-means clustering is superior to the k-Means technique [9]. The traditional FCM clustering algorithm has significant drawbacks [10] because it does not incorporate local neighbourhood information while clustering; it performs poorly for data clusters of different sizes and is vulnerable to outliers.

The Region of Interest (ROI) is intended to be separated from the remainder of the image. In this work, we use an improving clustering algorithm to determine the number of clusters and use an intuitionistic procedure incorporating spatial context to the fuzzy c means algorithm [11].

Firstly, we compute the number of clusters based on the breast tissue's parameter called mass quantity %; an optimal number of clusters should be given for processing image segmentation. The mass quantity percentage is the area of the predicted mass region by the total area of the breast tissue. The prediction of the mass region is calculated based on Morphological Area Gradient (MAG) [12]. Fig 3.10 shows the predicted mass region on the enhanced image using MAG; the green coloured in the (b) part shows the predicted segmented region, and the area of this region is divided by the whole breast area (i.e., complete area of the breast in (a)) is defined as mass quantity %. This quantity can estimate the number of clusters needed for the clustering method.

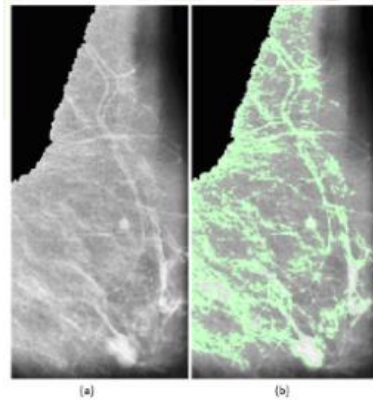


**Fig 3.10** (a) enhanced image from the previous step (b) Predicted mass region using MAG

Mass quantity % = 0.325, hence the number of clusters = 5

Based on this parameter value, the number of clusters for the images is divided into four categories:

- (i) Mass Quantity (MQ) % < 25 - number of clusters (n) = 4, (ii) 25 < MQ % < 50 - n = 5
- (iii) 50 < MQ % < 75 - n = 6, (iv) MQ % > 75 - n = 8

The fundamental component of MAG is the breast area's derivative to the pixel intensity, which quantifies how the area changes as a function of the intensity of the grey levels. The number of clusters computed here is used for the SIFCM algorithm.

#### A. SIFCM Clustering

FCM has been widely utilised in image segmentation because of its simplicity. The conventional FCM technique is prone to image artefacts because it considers only the grey value as a feature and ignores spatial information while clustering. We incorporate an intuitionistic spatial strategy to make the algorithm more resilient.

The main idea is based on Tripathy et al. [11] paper, with the optimal number of clusters being decided with the MAG algorithm, changes in neighbourhood kernel, Intuitionistic Fuzzy Set (IFS) representation, distance function and hesitation degree.

For nonspherical input data, the euclidean metric does not produce satisfactory results. We used altered Hausdorff distance as per [23] to fix this flaw. Between two groups of items, the Hausdorff distance [21] calculates the maximum of the minimum distance. This distance metric is used to compute cluster centres. A strong correlation exists between adjacent pixels in an image. A spatial function is established to use this criterion. A 9x9 equally (uniformly) weighted mask centred on the pixel has been applied. This work-built IFS using Yager's generator because it produces findings superior to Sugeno's [20].

Values are first randomly set for each cluster centre in the algorithm. After that, it converges to reduce the difference between the two iterations' cost function values and iterates until this difference is below the threshold value. This threshold was set at 0.01 to produce more accurate clusters.

#### B. Final Proposed Algorithm (SIFCM)

The segmented image is created by allocating pixels to clusters depending on the maximum membership value. The algorithm lists each stage of the suggested procedure.

Data: Input image, number of clusters determined by MAG, initial cluster centres.

Result: Image with each pixel assigned to a particular cluster

Step 1: Create an IFS image from the input image.

Step 2: On the IFS image, do modified spatial-intuitionistic fuzzy clustering:

Continue (repeat)

Calculate the membership values and determine the goal function's value.

Calculate the hesitation value and compute the membership.

Create a new membership function that takes the spatial function.

Use it to calculate the cluster centre value and update the cluster centre's value.

till  $\{J(\text{new}) - J(\text{old})\} < 0.01$ .

The third and final step is assigning the pixel to the cluster with the highest membership value. After SIFCM clustering, we need to filter the regions further to obtain the final detected mass.

### B) Filtering of regions for mass detection after SIFCM

Fig 3.11 shows the final image obtained after processing of SIFCM. For the image in Fig 3.11, the number of clusters obtained by the MAG technique is 5, and each pixel is assigned an index after clustering. Each index is coloured with a different colour.

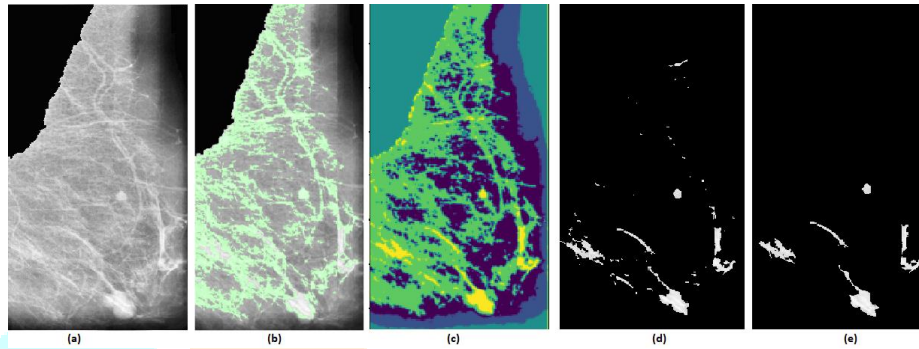


**Fig 3.11 - SIFCM processing**

- (a) Enhanced Image using wavelet-domain homomorphic filtering
- (b) Predicted mass using MAG - Mass Quantity % = 0.33, so the number of clusters=5
- (c) SIFCM processes the image with 5 clusters
- (d) Take the highest-intensity clustered index
- (e) Remove small regions that have an area<100 and keep only the regions that have an area>100.

We take the clustered index, which has maximum intensity. After taking the maximum intensity clustered region, we remove small, tiny spots by taking only the regions with an area>100, as shown in fig 3.11(e).

After removing small areas, as a part of the post-processing, erosion is executed to remove some extra lines that may come at the region's border. This helps remove some extra pixels on the border, and the identification of mass regions becomes easier. 5\*5 square kernel is taken for erosion with iterations=1.

After dilation, small regions whose area is less than 50 are removed. Then, we filtered some more regions using contour shape features such as eccentricity, rectangularity, and solidity. The ratio of non-zero pixels to the total number of zero pixels is used to calculate a new feature.

This post-processing phase excludes the regions with eccentricity less than 0.3 and more than 0.9 (these threshold values are determined experimentally). Breast lesions have a high solidity (measured as the proportion of the region's area to the area of the convex polygon around the region), resulting from their propensity to be round-like. Also, taking the height(h) and width(w) of the minimum bounding rectangle around the contour region, we calculated the parameter of dimensional ratio, i.e. minimum (h, w) divided by the maximum(h,w). The parts where it is of line-thread-like shape are removed by considering only the areas whose solidity is more significant than 0.4 and a dimensional ratio greater than 0.3. Fig 3.12 shows the image obtained after the post-processing stage (dilation followed by removal of regions based on shape features).

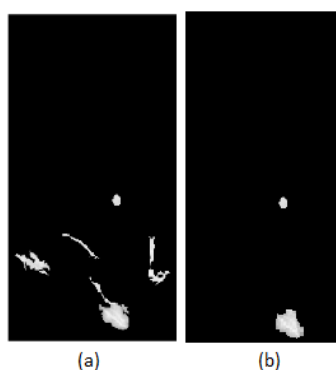


**Fig 3.12** Filtering of regions - (a) Maximum intensity clustered region after SIFCM on the enhanced image

(b) Final potential mass image after filtering.



In Fig 3.12(b), dilation is used after obtaining the clustered index region with maximum intensity as part of the post-processing. Then some regions are removed based on contour shape features like eccentricity, solidity, and rectangularity.

After filtering by contour features, we define another parameter to take the final region, potentially the lesion mass. First, draw the minimum bounding rectangle, as shown in Fig 3.13, around the mass; we calculate the number of non-zero(white) pixels in it and the number of zero(black) pixels in it, and the ratio as  $\text{number\_of\_non\_zero}/\text{number\_of\_zero}$ .

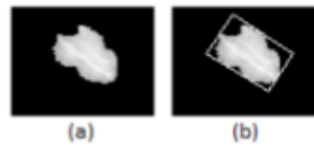


**Fig 3.13** (a) sample mass (b) minimum bounding rectangle

After drawing the minimum bounding rectangle, as shown in Fig 3.13(b), we calculate the number of non-zero and black(zero) pixels present inside this rectangle and compute the ratio. In the final image obtained after filtering by shape features like in Fig 3.12(b), further, we keep only those regions where the ratio is greater than 1. The regions whose ratio is less than one are removed. We take the maximum ratio obtained region as the mass lesion among the final masses.

In some cases, multiple masses are also present. If the number of regions in the filtered image exceeds 1, we take the top two maximum ratio obtained regions and compare their means. For instance, taking Fig 3.12(b), the number of regions is two, the ratio is computed for these two, and the means are compared. For this specific sample, the ratio is 3.1 for the smaller mass and 2.8 for the bigger mass. The mean value of a smaller mass is 216, and that of a bigger mass is 220. If the mean difference is less than ten and the ratio difference is less than 0.5, then we consider the second mass. In this case, we take both masses as the difference between their ratios and means is less. We only take the maximum ratio region if the difference is more.

#### IV. Dataset and Experimental Results

##### 4.1 Dataset - Mini-MIAS database

For segmentation analysis, mammogram breast medical images were taken from the Mammography Image Analysis Society(mini-MIAS) database [22]. The region of interest is described as the circle where the centre and the radius are given. These ROIs are compared with the obtained ROIs to calculate the accuracy. There are a total of 322 images in this database.

##### 4.2 Results and Discussions

Table I. Comparitive analysis with an existing literature				
Author	Methodology used	Number of images tested(Mini-MIAS)	Accuracy	Remarks
Vikhe et al.	Wavelet processing and the piecewise linear operator	45	90.9	Only 45 images are tested. It detects only masses
Mahfuzah et al.	Chan-Vese technique	30	90	Only 30 images are tested. It detects only masses
Soulami et al	Electromagnetism like optimization	56	78.57	It did not work well for Dense Mammograms.
Hongyu et al	Gestalt psychology	257	92	Mind and Behaviour is taken into consideration
Asaad Zebari et al	Hybrid thresholding	322	78.88	It detects only masses
Ayush Shrivastava et al	Sliding Window, Dispersed Region growing	322	91.3	In pectoral removal, sliding window does not work well for all mammograms because breast organ size and intensity varies from one to another mammogram. In mass detection,dispersed region growing is a time consuming task to detect seeds
Proposed	Automated detection of masses and microcalcifications in Pectoral removed MLO mammograms with image enhancement and modified Fuzzy C-means	322	94.72	This approach detects both masses as well as microcalcifications and all images of mini-mias are tested(322/322)

The proposed algorithm accurately segmented 305 mammographic images, and the remaining 17 photos deviated from the right ROI, yielding an accuracy of 94.72%. We should note that direct comparisons are challenging because several authors judged their approaches using the radiologist's visual evaluation. Another issue is that inconsistency in the data sets used (such as the no. of images) and assessment measurement kinds.

The proposed algorithm's strength is that it has been tested on all dataset images. Finding the impacted breast area is our research's major objective. Some research focused only on tumour detection and avoided calcifications in the breast. Regarding our work, all breast tumours and calcifications are examined with separate enhancement and detection methods. Table I shows that we outperformed earlier segmentation techniques and achieved better results.

#### V. CONCLUSION AND FUTURE WORK

In this paper, we proposed an approach to detect mass and microcalcifications. Before the detection, enhancement algorithms are also executed to improve visual quality and mass isolation. The first one is enhancing images with Nonsubsampled contourlet transform images to improve the visibility of calcifications and detect them by morphological operations. The second one is strengthening the image with wavelet-based homomorphic filtering and CLAHE to enhance mass regions and improving contrast and clustering with Spatial Intuitionistic fuzzy C-means (SIFCM). The different treatment of microcalcifications is frequently disregarded, which was important for our suggested segmentation technique. In future, we will work on classification of masses.

## REFERENCES

- [1] <https://www.mskcc.org/cancer-care/types/breast/anatomy-breast>
- [2] <https://breast-cancer.ca/mammopics/>
- [3] Ch.Sarada, Dr K.Vijaya Lakshmi, Prof. M.Padmavathamma(2022) Pectoral Removal from MLO Mammogram: Ensemble of adaptive MSERPectoral and SlopeEdgeDetection with extensive Pre-processing. Samriddhi: A Journal of Physical Sciences, Engineering and Technology
- [4] José Muñoz, Domínguez, Villegas, Sánchez and Leticia Maynez-The Nonsubsampled Contourlet Transform for Enhancement of Microcalcifications in Digital Mammograms: MICAI 2009, LNAI 5845, pp.292-302, 2009
- [5] Michael Wirth, Matteo Frascini, Jennifer Lyon (2004) Contrast enhancement of microcalcifications in mammograms using morphological enhancement and non-flat structuring elements
- [6] Smallest enclosing disks (balls and ellipsoids), Emo Welzl, 1991
- [7] He Wen, Wu Qi, Li Shuang (2016) Medical X-ray Image Enhancement Based on Wavelet Domain Homomorphic Filtering and CLAHE, 2016 International Conference on Robots & Intelligent System
- [8] Donoho, David L.; Iain M. Johnstone (December 1995). "Adapting to Unknown Smoothness via Wavelet Shrinkage". Journal of the American Statistical Association.
- [9] Wiharto W, Suryani E. The Comparison of Clustering Algorithms K-Means and Fuzzy C-Means for Segmentation Retinal Blood Vessels. Acta Inform Med. 2020 Mar
- [10] Memon, K. H., Lee, D. H.: 'Generalised fuzzy c-means clustering algorithm with local information, IET Image Process, 2017
- [11] B. K. Tripathy, A. Basu and S. Govel, "Image segmentation using spatial intuitionistic fuzzy C means clustering," 2014 IEEE International Conference on Computational Intelligence and Computing Research
- [12] G. F. Torres et al., "Morphological Area Gradient: System-independent Dense Tissue Segmentation in Mammography Images," 2019 41st Annual International Conference of the IEEE Engineering in Medicine and Biology Society (EMBC)
- [13] Vikhe PS, Thoo VR (2016) Mass detection in mammographic images using wavelet processing and adaptive threshold technique. J Med Syst 40(4):82.
- [14] Mustafa, Mahfuzah & Rashid, Hana & Abdullah, Nor Rul Hasma & Samad, Rosdiyana & Pebrianti, Dwi. (2017). Mammography Image Segmentation: Chan-Vese Active Contour and Localised Active Contour Approach. Indonesian Journal of Electrical Engineering and Computer Science.
- [15] Mohammed Y. Kamil, Ali Mohammed Salih "Mammography Images Segmentation via Fuzzy C-mean and K-mean" INASS publication, 2018.
- [16] Soulam KB, Saidi, Honnit, Anibou, Tamtaoui (2018) Detection of breast abnormalities in digital mammograms using the electromagnetism-like algorithm. Multimedia Tools. Suckling J, Parker.
- [17] Wang H, Feng J, Qirong B et al. (2018) Breast mass detection in digital mammogram based on gestalt psychology. Journal of Healthcare Engineering (J HEALTHC ENG) 2018: Article ID 4015613.
- [18] Diovan, Ibrahim, Zeebaree, Mazin, Haron, Asaad Zebari, Robertas and Maskeliunas(2021) Breast Cancer Detection Using Mammogram Images with Improved Multi-Fractal Dimension Approach and Feature Fusion
- [19] Ayush Shrivastava, Arpit, Devang, Vibhav Singh, Rajeev Srivastava "Automated Digital Mammogram Segmentation Using Dispersed Region Growing and Sliding Window Algorithm" 2017 IEEE conference on Image, Vision and Computing.
- [20] T. Chaira, A novel intuitionistic fuzzy C means clustering algorithm and its application to medical images, Appl. Soft Comput. 11 (2011), 1711–1717.
- [21] W.-L. Hung and M.-S. Yang, Similarity measures of intuitionistic fuzzy sets based on Hausdorff distance, Pattern Recogn. Lett. 25 (2004), 1603–1611.
- [22] <http://peipa.essex.ac.uk/info/mias.html>
- [23] Aruna Kumar, S.V. and Harish, B.S. "A Modified Intuitionistic Fuzzy Clustering Algorithm for Medical Image Segmentation", *Journal of Intelligent Systems*, vol. 27, no. 4, 2018, pp. 593-607.